nature reviews earth & environment

https://doi.org/10.1038/s43017-022-00373-x

Technical review

Check for updates

Landslide detection, monitoring and prediction with remote-sensing techniques

Nicola Casagli, Emanuele Intrieri ✉, Veronica Tofani, Giovanni Gigli & Federico Raspini

Abstract

Landslides are widespread occurrences that can become catastrophic when they occur near settlements and infrastructure. Detection, monitoring and prediction are fundamental to managing landslide risks and often rely on remote-sensing techniques (RSTs) that include the observation of Earth from space, laser scanning and ground-based interferometry. In this Technical Review, we describe the use of RSTs in landslide analysis and management. Satellite RSTs are used to detect and measure landslide displacement, providing a synoptic view over various spatiotemporal scales. Ground-based sensors (including ground-based interferometric radar, Doppler radar and lidar) monitor smaller areas, but combine accuracy, high acquisition frequency and configuration flexibility, and are therefore increasingly used in real-time monitoring and early warning of landslides. Each RST has advantages and limitations that depend on the application (detection, monitoring or prediction), the size of the area of concern, the type of landslide, deformation pattern and risks posed by landslide. The integration of various technologies is, therefore, often best. More effective landslide risk management requires greater leveraging of big data, more strategic use of monitoring resources and better communication with residents of landslide-prone areas.

Sections

Department of Earth Sciences, Università degli Studi di Firenze, Florence, Italy. ✉e-mail: emanuele.intrieri@unifi.it

Introduction

Landslides are ubiquitous in sloping environments and can be driven by tectonic[1], climatic[2] or human[3] activities (Box 1). Landslide disasters arise when the hazardous movement of soil and rocks directly or indirectly impacts vulnerable human settlements and infrastructure, sometimes causing widespread damage. Between 2004 and 2016 alone, an estimated 55,997 people were killed worldwide in 4,862 distinct landslide events (not counting those caused by earthquake), with Asia being the most affected continent[4].

Landslide risks could be exacerbated by global changes such as increases in the frequency or magnitude of rainfall and permafrost degradation[5]. As such, international organizations and agencies promote landslide risk reduction policies that include understanding risks and enhancing disaster preparedness for effective response. The 2020 Landslide Kyoto Commitment, for example, aims to provide the tools, information, platforms, technical expertise and incentives to promote landslide risk reduction on a global scale.

To achieve these goals, it is vital to detect the presence, monitor the velocity and predict the stability conditions of unstable slopes and the evolution of these features with time. However, the complex and widespread nature of landslides necessitates accurate measurements, often with a spatial coverage capable of targeting one or more slopes and an acquisition frequency high enough to catch substantial changes in the landslide (depending on the type of landslide; Box 1). In situ monitoring techniques are generally not suitable for wide-area monitoring, as each single sensor provides information only concerning its surroundings, and can require the operators to enter hazardous or inaccessible areas. Remote-sensing techniques (RSTs) have therefore become an indispensable tool in landslide investigation[6], as they offer a systematic, synoptic and cost-effective view of the ground surface at various scales. The use of RSTs has enabled a greater understanding of the complex interaction between different geological and geomorphological phenomena underlying disruptive processes[7,8].

Broadly, RST includes tools that do not require human contact with the target and can be space-borne or ground-based, both of which are used in landslide science. For example, satellite RSTs are extensively used in landslide monitoring, with their use growing since the 2000s owing to continuous technological advancements, such as the development of algorithms to substantially improve the quality of monitoring data[9] and the launch of satellites with increasingly higher acquisition frequency and spatial resolution[10,11]. Ground-based laser scanning is widely used for slope instability detection, mapping and monitoring[12–14]. Some techniques can be applied from either platform. For example, since the 1990s, satellite-based sensors have used interferometry, which can measure how much a target is moving with sub-millimetre accuracy. Since the 2000s, interferometry has also been used applying ground-based apparatuses, allowing for more tailored applications. Since the advent of RSTs, the capability to rapidly map landslides over wide areas[15], to collect information that provides mechanistic and kinematic insight[16,17] and to gather big data for issuing early warnings[18] has considerably increased.

In this Technical Review, the potential and application of RSTs for landslide detection, monitoring and time prediction are discussed. We mainly focus on multispectral and interferometric satellites, ground-based interferometry, laser scanning and Doppler radar, which have been increasingly used among the RSTs developed since the early 2000s. RST function and development in landslide science are described, followed by an overview of their application, advantages and limitations in detection, monitoring and forecasting. Finally, we present future directions for research and development to best improve their usage in landslide risk management.

Space-borne techniques

Since the launch of Landsat-1 in 1972, RSTs were recognized as a promising tool for landslide study[6,19] as they provide systematic, large extent information of different parameters of the land surface, enabling investigation of active disruptive processes at different spatial and temporal scales[7,8]. Currently, the study of landslides with various geometries, styles and kinematics is enabled by the availability of sensors operating at different wavelengths and frequencies, which offer different spatial, temporal and spectral resolutions[20]. Modern landslide analysis also benefits from imagery collection within the multispectral[21,22] and microwave[10,23] domains of the electromagnetic spectrum. For example, both very-high-resolution (VHR) multispectral and synthetic aperture radar (SAR) satellite acquisitions have been exploited to compile landslide databases[24] and to measure and quantify ground deformation induced by the occurrence of landslides[25]. Characteristics of space-borne multispectral and radar sensors and basic processing principles are described in this section.

Multispectral satellite sensors

Satellite images acquired in the visible, near-infrared and shortwave infrared spectrum have been largely used for producing landslide inventory maps, often with a regional scale of analysis[26]. In most cases, multispectral images are used for mapping terrain features indicative of the occurrence of landslides, such as surface landforms, geological structure, land-use practices, distribution of vegetation[24] and temporal changes of these factors[27].

Multispectral satellite platforms (such as Landsat, ASTER, SPOT and Sentinel-2) host passive instrument payloads capable of detecting and measuring reflected or emitted electromagnetic radiation from the surface of Earth[28] (Fig. 1a). They observe Earth perpendicularly to the orbital track following sun-synchronous trajectories, to ensure that the angle of sunlight on the surface of Earth is consistently maintained. Acquisition time, selected to minimize the potential impact of shadows and to guarantee a suitable level of illumination, is usually in the morning (the mean local solar time at the descending node is 10:30 for Sentinel-2). The acquisition time of the day is quite close for most of the missions (Landsat, SPOT and WorldView-3); to make it so different, archives and existing and historical missions are comparable and therefore can be integrated. This feature is important, for example, when trying to reconstruct the past activity of a landslide as it minimizes the needs to apply corrections for different shadow angles and light conditions.

There are several considerations in selecting satellite data for use in landslide research. For instance, the revisiting time is highly variable between satellites, ranging from a daily basis (WorldView and Pléiades constellations) to a few days (QuickBird-2 and GeoEye-1) to weeks (16 days by the Landsat family and 26 days by SPOT-5). A substantial improvement in temporal observation frequency is provided by the adoption of virtual constellation of mid-resolution multispectral satellites[29]. Jointly, Landsat-8 and Landsat-9 (a repeat cycle of 8 days) and Sentinel-2a and Sentinel-2b (a repeat cycle of 5 days) provide a global median average revisit interval of 2.3 days[30].

The swath width (or footprint) also varies between sensors, ranging from several kilometres for VHR satellites (about 13 km for WorldView-3 and WorldView-4) to 120 km for SPOT-5, 185 km for Landsat-7 and 290 km for Sentinel-2. Ground sampling distance varies depending

on the particular spectral band, generally increasing from the visible and the near infrared to the shortwave infrared. The launch of VHR satellite systems, which usually cover the visible bands and include panchromatic domain (blending the information of blue, green and red bands), led to the acquisition of images with 0.25 m up to 1 m ground sampling distance. For VHR satellites (for example, GeoEye-1 and GeoEye-2, QuickBird-2, Cartosat, WorldView-3, Pléiades-1 and Pléiades-2 and IKONOS), panchromatic imaging capability at nadir is about four times finer than that of the multispectral band[31]. There are many pan-sharpening algorithms[32] for merging low spatial resolution multi-spectral images with higher spatial resolution panchromatic bands to generate a single high-resolution colour image. However, data fusion of different spatial and spectral resolution can impact on the characteristics of the image useful for landslide detection and mapping, such as linear features, textures, contrast and colour[33].

The current availability of different satellite platforms increases the possibility to timely acquire cloud-free multispectral imagery following a major landslide event or during a period of high deformation, when monitoring landslide activity and predicting its possible failure must be rapidly carried out. Nevertheless, weather conditions (especially clouds and snow cover) and daylight can still hamper the acquisition of suitable images, depending on the climate zone and the season. In general, mountain areas and areas with humid climates and rainy seasons are potentially the most unfavourable regions and times for optimal images. Unfortunately, these are often the times and places when landslides are more likely to occur, representing a major limitation to this technology.

Box 1

Landslide classification

Landslide is an all-inclusive term referring to downward and outward movement of slope-forming materials under the influence of gravity[157], which can ubiquitously act on both natural, and engineered and excavated slopes[158]. Landslides can occur in slopes on the verge of instability and can be triggered by natural processes (rainfall, snowmelt, erosion by stream, volcanic activities and earthquake shaking), human disturbances (agriculture, construction, mining, cuts or variation of reservoir levels) or any combination of these factors.

Landslides can be initiated by both intense, short-duration rainstorm events (hours to days) and long-lasting precipitation (weeks to months), leading to longer timescale seasonal fluctuations[159]. The first events commonly trigger shallow slides, whereas the second episodes are normally associated with deeper and larger slope movements (5–20-m depth). Deep-seated and shallow landslides intrinsically differ in their volume, extent, hydrological triggering[160], occurrence[161] and the risk posed.

One of the most widely used classifications is based on the type of movement (falls, topples, slides, spreads, flows and complex) and the type of material involved (rock, debris and earth)[162], with a velocity scale (later updated[86]) completing the scheme (see the table). An updated classification proposes a matrix with 32 landslide types[163]. However, classification schemes are not perfect, as the type of movement and material varies in space and time, and an almost continuous gradation of types exists.

Description	Typical velocity	Probable related destruction
Extremely rapid	5 m s^{-1}	Major catastrophe; buildings destroyed; high causality rate as escape unlikely
Very rapid	3 m min^{-1}	Some lives lost, velocity too great to permit everybody to escape
Rapid	1.8 m h^{-1}	Escape evacuation possible; structures and possessions destroyed
Moderate	13 m per month	Some temporary and insensitive structures can be temporarily maintained
Slow	1.6 m per year	Remedial construction can be undertaken during movement; insensitive structures can be maintained with frequent work if the total movement is not large during an acceleration phase
Very slow	16 mm per year	Some permanent structures undamaged by the movement
Extremely slow	<16 mm per year	Imperceptible without instruments; construction possible with precautions

SAR satellite sensors

Unlike passive remote sensing, active sensors such as SAR instruments[34] provide their own energy source for illumination. As a result, they are able to obtain measurements anytime, regardless of the time of day or season, using bands of the microwave domain[35]. This feature is critical for continuous landslide monitoring and prediction.

A SAR image is composed of pixels corresponding to a ground area characterized by amplitude and phase values. Although amplitude depends on the reflectance of the illuminated objects, phase value of a single SAR image partly depends on the sensor–target distance – when a point on the ground moves, the distance between the sensor and the point changes and the phase value recorded by the sensor is affected accordingly. This feature is the key element in interferometric applications, a wide term referring to the exploitation of the SAR signals of at least two SAR images[36]. The spatial resolution of SAR images depends on the sensor used and its acquisition mode. The temporal resolution depends on the revisiting time of the satellite and ranges from several weeks (Radarsat constellation) to a few days (Sentinel-1 constellation). A suitable approach to exploit phase variation between two consecutive radar images acquired over the same target area is the differential interferometric SAR (DInSAR). After topography compensation, DInSAR enables the measurement of surface motions from several dozens of centimetres to 1 cm or less (depending on the wavelength) with suitable resolution over areas of tens or hundreds of squared kilometres[37].

Atmospheric phase distortions[38] and geometrical and temporal decorrelation[39] reduce (or even compromise) the quality and reliability of DInSAR results. To overcome these limitations, interferometric SAR (InSAR)-based information can be enhanced through multitemporal interferometric SAR (MTInSAR) approaches, based on the analysis of long stacks of coregistered SAR imagery[9,40–43]. MTInSAR is designed to identify a grid of measurement points (MPs) corresponding to a single pixel or a group of few pixels exhibiting a stable radar signature over the entire observation period (Fig. 1b). MPs usually correspond to man-made objects, rocky outcrops and bare soil, which are characterized by high reflectivity and stability (movements not higher than few tens of centimetres per year). For each MP, it is possible to estimate displacement time series along the satellite line of sight (LOS) and a set of quality parameters. LOS deformation rate can be estimated with

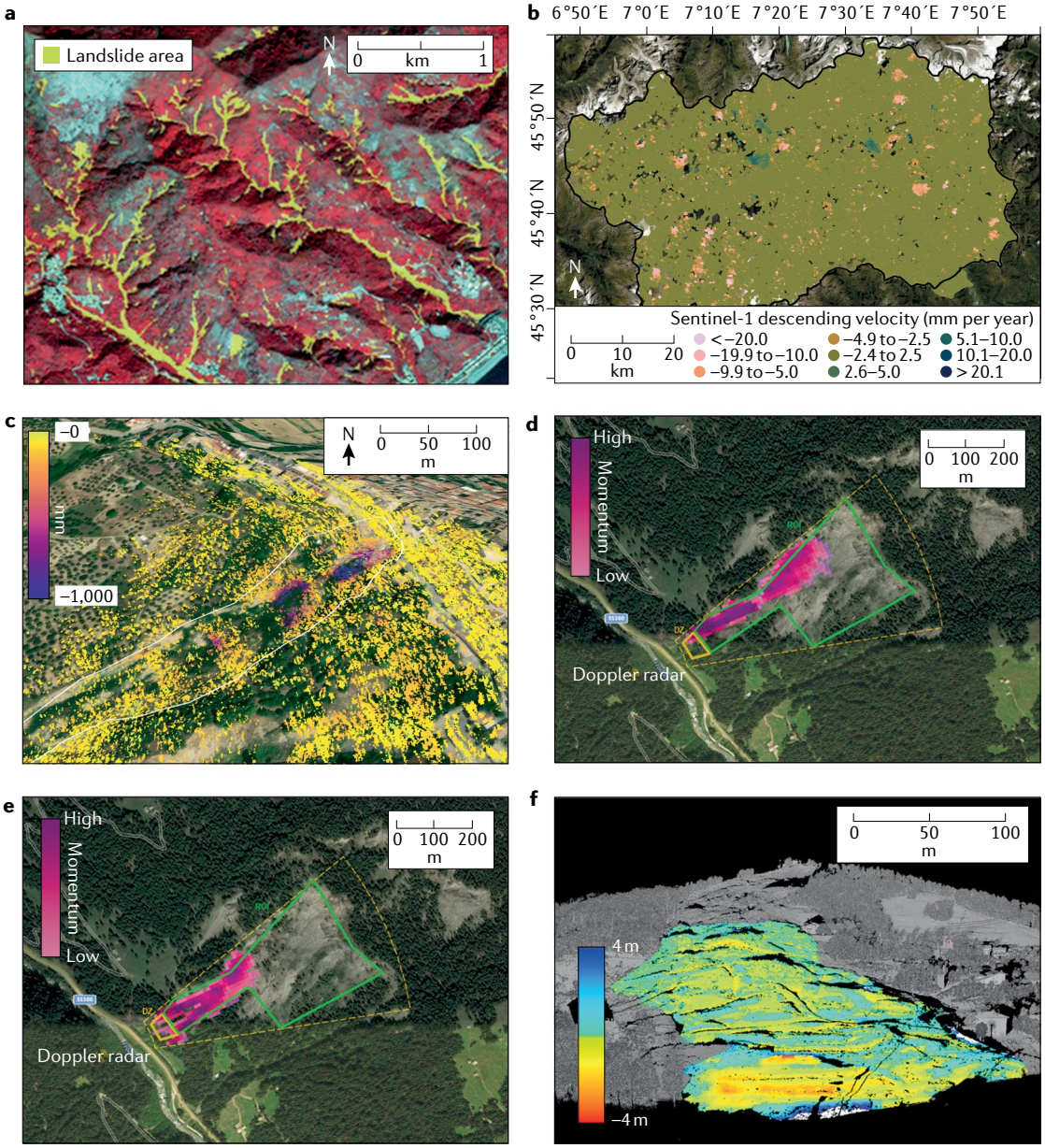

Fig. 1 | Landslide remote-sensing products. a, QuickBird imagery in the multispectral very-high-resolution analysis of the Giampilieri area, Italy, which had more than 600 landslides following a storm. The image is represented in false colours, in which the red areas are those with a high reflectivity in the near-infrared spectrum (that is, vegetated areas), the cyan areas are bare soil or cities and the yellow areas are the pre-event and post-event differences, indicating landslides (from ref.[11]). **b**, Deformation map of the Val d'Aosta region, Italy, elaborated using multitemporal interferometric synthetic aperture radar Sentinel-1 data acquired along the ascending orbit of the satellite. **c**, Displacement map of the landslide of Pomarico, Italy, from a ground-based interferometer and projected over a multispectral image. Yellow pixels were stable over 30 months; the purple shows movement towards the sensor owing to a landslide. **d**, Product of a Doppler radar applied on a rock avalanche threatening a street in Ruinon, Italy, on 12 September 2020. The dashed yellow area is the Doppler radar field of view. The colour bar indicates the local intensity of the detected rockfall using an arbitrary scale that is a proxy of the momentum of the landslide. The full green line denoted as ROI (region of interest) includes the area of potential movement. If the collapsing material enters the area called DZ (danger zone), delimited by the full yellow line, then a warning is issued. **e**, As in **d**, but for 1 October 2020. **f**, Comparison of two lidar scans of the Marano landslide, an earth flow in Italy, that were acquired 5 days apart. The cool colours represent earth advance and the warm colours denote a retreat. Part **a** is reprinted from ref.[11], CC BY 4.0 (https://creativecommons.org/licenses/by/4.0/).

an accuracy theoretically lower than 0.1 mm per year, at least for very stable MPs during a long time span, whereas the accuracy of the single measurement in correspondence of each SAR acquisition ranges from 1 to 3 mm (ref.[44]). A high accuracy is important when measuring the movement of extremely slow landslides (Box 1) that would otherwise be detectable only after several months of cumulated displacement.

Analysis of amplitude information is an effective alternative to InSAR for mapping surface deformation in the case of temporal decorrelation[45] or loss of coherence[46]. Amplitude-based methods exploit the correlation of the speckle pattern of two images (pre-landslide and post-landslide failure, for instance). If the deformation introduces geometric distortions without substantially affecting the SAR image reflectivity, by tracking amplitude features in multitemporal SAR data, movement rates (from tens of centimetres to tens of metres) exceeding those observables with InSAR can be recorded. Despite a lower precision (of the order of 1/50th to 1/20th of the image pixel)[47], speckle tracking offers all the three geometrical components (x, y and z) of the displacement vector, having images acquired along ascending and descending orbits.

Analysis of phase and amplitude collected by radar sensors is a powerful tool for landslide investigation, especially over large areas, allowing for the retrieval of information about distinct displacement regimes, ranging from small to high deformation rates. A general drawback of space-borne applications is that they are not customizable; acquisition parameters such as acquisition frequency are fixed and typically of the order of a few days, and shadows — affecting steep slopes, narrow valley and certain orientations in particular — reduce the amount of ground surface reflecting the signal. For example, for space-borne InSAR, north–south facing slopes are unfavourable as supposed movements along such slopes would be roughly perpendicular to the LOS and therefore undetectable. As a result, specific locations might not be optimally studied with satellite platforms and could require a more tailored approach using ground-based sensors.

Ground-based techniques

Although satellites scan wide areas and spot unstable zones, terrestrial remote-sensing technologies monitor single slope instabilities for short-to-long-term landslide management. By exploiting radar, laser and multispectral signals, ground-based technologies can be versatile, accurate and precise, with high spatial and temporal resolution. For example, ground-based InSAR (GBInSAR) can take less than 1 min (up to 10–20 s for some apparatuses). This (at least) tenfold improvement means that landslides up to the boundary between moderate and rapid velocities can be monitored (Box 1). This section describes ground-based interferometry, Doppler radar and lidar in landslide monitoring.

Ground-based interferometry

Ground-based interferometry was born in mid-1990s following the observation that the technique developed on satellite platforms would have been useful to measure slope deformations[48] and man-made structures such as dams[49]. Ground-based apparatuses are developed to use both synthetic (such as GBInSAR) and real aperture radar. In the latter case, dish antennas are used to make acquisitions over small (a few squared metres) areas and are then rotated and pointed at the adjacent resolution area until the whole scenario of interest is scanned; therefore, the acquisition time is a function of the extension of the monitored area. The acquisition time for GBInSAR is related to the length of the synthetic aperture, which is usually obtained by moving back and forth the antennas along a linear rail (generally 2–3 m long). Both systems are capable of near real-time slope-scale monitoring, with potential for early warning, as they produce nearly spatially continuous displacement data (displacement maps) (Fig. 1c), with deformation rates ranging from a few millimetres per year up to several metres per day. Similarly, they both can achieve sub-millimetre precision and a spatial resolution in the order of 1–10 m. They also perform an acquisition in less than 2 min (at least considering a 30–45° horizontal field of view), operate fully remotely and ensure 24-h operativity in nearly all-weather conditions (although strong wind, rainfall and high air temperature and humidity gradients can generate noise). These features are key to providing landslide warnings.

The flourishing of various applications and the continuous technological evolution of such systems demonstrate that ground-based interferometry is a cutting-edge approach for landslide monitoring and prediction. Uses have been successfully trialled dating back to the early 2000s, including monitoring and early warning of landslides threatening public safety[16,50], unstable slopes in open-pit mines[51,52], the flanks of volcanic edifices[53], the residual slope risk after collapse[54] and assessing the effectiveness of stabilization works[17].

Doppler radar

Some types of rapid landslides, such as rockfalls and debris flows, often lack notable precursors. Therefore, risk mitigation strategies are usually focused on active or passive defence structural works and can use tools to detect the ongoing collapse; one such tool is a sophisticated radar system that exploits the Doppler effect principle. These devices enable effective real-time monitoring, so that alerts are issued during the event itself. As the moving mass of earth is often situated along a slope at a higher altitude than the elements exposed to risk, this real-time monitoring can provide a lead time of some tens of seconds, which could be sufficient to automatically turn off a traffic light and close a street or trigger a siren to clear the area and allow people to reach a safe location.

The first successful attempts to combine rapid mass movement detection and road closure with medium-range Doppler radar techniques were made on snow avalanches[55]. After that, a long range, wide-angle, radar-based avalanche detection system that is integrated into a fully operational warning system has been developed to detect avalanches and to close threatened roads without human intervention[56]. Since the late 2010s, the Doppler radar technique has been successfully adapted and implemented on debris flow[57,58] and rockfall monitoring and early warning systems[59–61].

The operating principle[62] consists in the emission of an electromagnetic signal in the microwave domain by a frequency-modulated continuous wave radar sensor. The signal reflected by the surrounding scenario is picked up by multiple receiving antennas and analysed to determine the occurrence of rapidly moving objects along the observed slope. If the object dimension and velocity are large enough, a deviation in the signal frequency, or Doppler effect, is induced and detected. Owing to its ability to provide 2D maps of rapid events, including the measurement of their velocity, duration and trajectories, Doppler radar represents an operative tool to detect and track rapid landslides (faster than 1 m s^{-1}) and to issue alarms.

Detection warnings can be customized according to appropriate spatial criteria and need to be filtered using specific algorithms to discriminate true events from false alarms (such as those owing to atmospheric disturbances or to tree top oscillation). The system is, therefore, able to measure in real time the landslide speed and to precisely geolocalize its propagation trajectory (Fig. 1d,e). It is possible to detect the presence of bodies larger than some cubic metres that move faster than a few metres per second at about 1–2 km from the sensor. Several simultaneously occurring events can also be tracked, provided that they are at least 10 m far from each other. Alarm notifications (SMS and e-mail) are sent by the control unit associated with the radar sensor; the system can also be connected to safety devices such as traffic lights, sirens or self-closing bars. This solution can be particularly convenient in the case of roads at the base of rocky walls or detrital slopes affected by widespread and repeated instability phenomena.

Lidar

Lidar techniques are used for monitoring unstable slopes as they provide detailed digital models of the observed surface over which other spatial information can be projected (such as interferometric displacement maps), information on the volume of an event and, if multiple scans taken at different times are compared, a displacement field can be detected and monitored (Fig. 1f). They enable 3D landslide analysis by using a narrow laser beam to scan a certain object according to a pre-defined scanning pattern. The direct output of the laser scan is a cloud of points, the positions of which are expressed in polar coordinates referred to the centre of the device. For a specific angular resolution, the resulting point density is therefore a function of the laser shooting distance. Point clouds can be analysed to generate the 3D model of the landslide. Instruments used for ground surveying and monitoring are mainly based on the time-of-flight measurement for distance calculations and have maximum ranges from a few hundred metres up to a few kilometres[13].

Lidar systems can be used from a fixed position on the ground (terrestrial lidar), or they can be mounted on mobile platforms, such as aeroplanes (aerial lidar), drones, cars and boats (mobile lidar). As the distances are referred to a fixed reference system that is centred on the instrument, terrestrial lidar does not require positioning correction systems. This feature reduces the elaboration time and prevents the need for a global navigation satellite system to record coordinates. Most commercial lidar sensors record from one to up four echoes of the reflected pulse, which makes it possible to distinguish different return pulses deriving from objects placed at different ranges (vegetation and ground) for the same emitted pulse. In addition, full waveform lidar systems are able to digitize the complete return waveform[63], giving access to an almost unlimited number of returns per shot and high multiple-target resolution, thus increasing details on canopy, sub-canopy structures, ground vegetation and ground morphology.

The spatial resolution of aerial lidar is a function of the altitude and flight speed, ranging from a few centimetres for altitudes of about 250 m to a few decimetres for flight altitudes higher than 1,000 m. Data accuracy depends on the accuracy of the devices used for movement compensation. Thus, aerial lidar is particularly suitable when a large area needs to be covered, or if the investigated slope is too far to be observed from a terrestrial position. For an optimal panoramic viewpoint, terrestrial lidar provides higher accuracy and resolution, especially on steep and overhanging slopes.

Applications

Both space-borne and ground-based RSTs are key in the three main steps required in the instrumental management of landslides hazard (detection, monitoring and prediction). The RSTs described in the previous section are evaluated here under the lenses of these applications. There is not a single technique outperforming the others in all the fields, and performances depend on technical parameters, such as spatial resolution, extension of the investigated area, operating distance, acquisition frequency, accuracy and detectable velocity, that vary with each sensor (Fig. 2). The choice of the most appropriate instrument (or instruments) also depends on the type of application in relation to the type of landslide, as any landslide type is generally associated with a characteristic range of possible volumes, velocities and other features such as type of trigger, geomechanical properties and topography, which make some tools more suitable than others (Table 1).

Detection

Landslide detection consists in the collection of data and information on the presence, distribution and intensity of landslides and the identification of elements affected by the deformative process. Multispectral imagery is mostly used in the detection of already occurred landslides, which can be apparent on the ground but still needs to be identified, mapped and classified, for example, to provide support to post-emergency activities such as damage assessment and reconstruction. The use of multispectral imagery has benefitted from increasing computing capacity, improvement in analysis and visualization software and the flourishing of cloud platforms for processing. The increased availability of HR and VHR sensors has also had an important role in overcoming the low spatial resolution of many existing sensors[64]. Classification models applied to VHR panchromatic and HR multispectral satellite images have proven to be valuable for detection and mapping rapid rainfall-induced landslides over large areas[65]. Automatic methods for landslide mapping can be grouped into two main classes: whether they perform a pixel-by-pixel analysis to detect colour or luminosity variations between pre-event and post-event images (pixel-based approach), or whether the basic unit of this analysis is conducted on a group of pixels defining meaningful shapes (object-based approach).

When detection is not made on slowly moving landslides (not already collapsed areas), it is often carried out by measuring the ground displacement with InSAR techniques. For example, satellite DInSAR has been widely used since the 1990s[66,67] to measure the spatial extent and the magnitude of surface deformation associated with mass movements[68–71]. Satellite-based InSAR can be used to detect and map landslides in remote areas, in mountainous terrain and/or, in general, where deployment of ground-based tools is not logistically feasible and in situ activities are challenging. This aspect is important in mapping landslides without previous knowledge of their location[72], and particularly for areas with permafrost[73] or seasonally frozen ground[74], whose susceptibility to geohazards, including landslides, is expected to increase with rapid warming[75,76]. Indeed, since the early 2000s[23], InSAR has been profitably used to study landslides, becoming a consolidated tool used at different scales – from national[77] to regional[78], basin[79], single slope[80] and building[81] – as well as in different phases of landslide response and Civil Protection practice[82]. The ability to make numerous MPs over the landslide body allows for the detection and mapping of the actively deforming slopes[83], the characterization of landslide mechanism[84], the zonation of sectors with different velocities and behaviours within the landslide area[85] and the modelling of large slope instability[69].

MTInSAR, in particular, is highly effective in the analysis of landslide-related events at different stages[26], although it is restricted to 'coherent' landslides, which have little internal deformation and with extremely slow and very slow movements[86] (Box 1). Over natural, rural and mountainous areas, MTInSAR results are impacted by effects that reduce the intensity and stability of the microwave signal, especially the fast and chaotic movements of the vegetation. In these settings, exploitation of long wavelength (such as L-band) can lead to the generation of more reliable displacement maps[87] and the retrieval of higher spatial density of MPs[88] than short wavelength (such as C-band), owing to its ability to penetrate through a tree canopy surface. However, processing and interpreting SAR data can be challenging[89] in alpine environments, which are characterized by high topographic gradients and persistent snow cover. SAR amplitude-based and pixel-offset techniques[90,91] are a valid method to map the deformation induced by rapid landslides in a vegetated area and where rapid changes impair the InSAR approach[92].

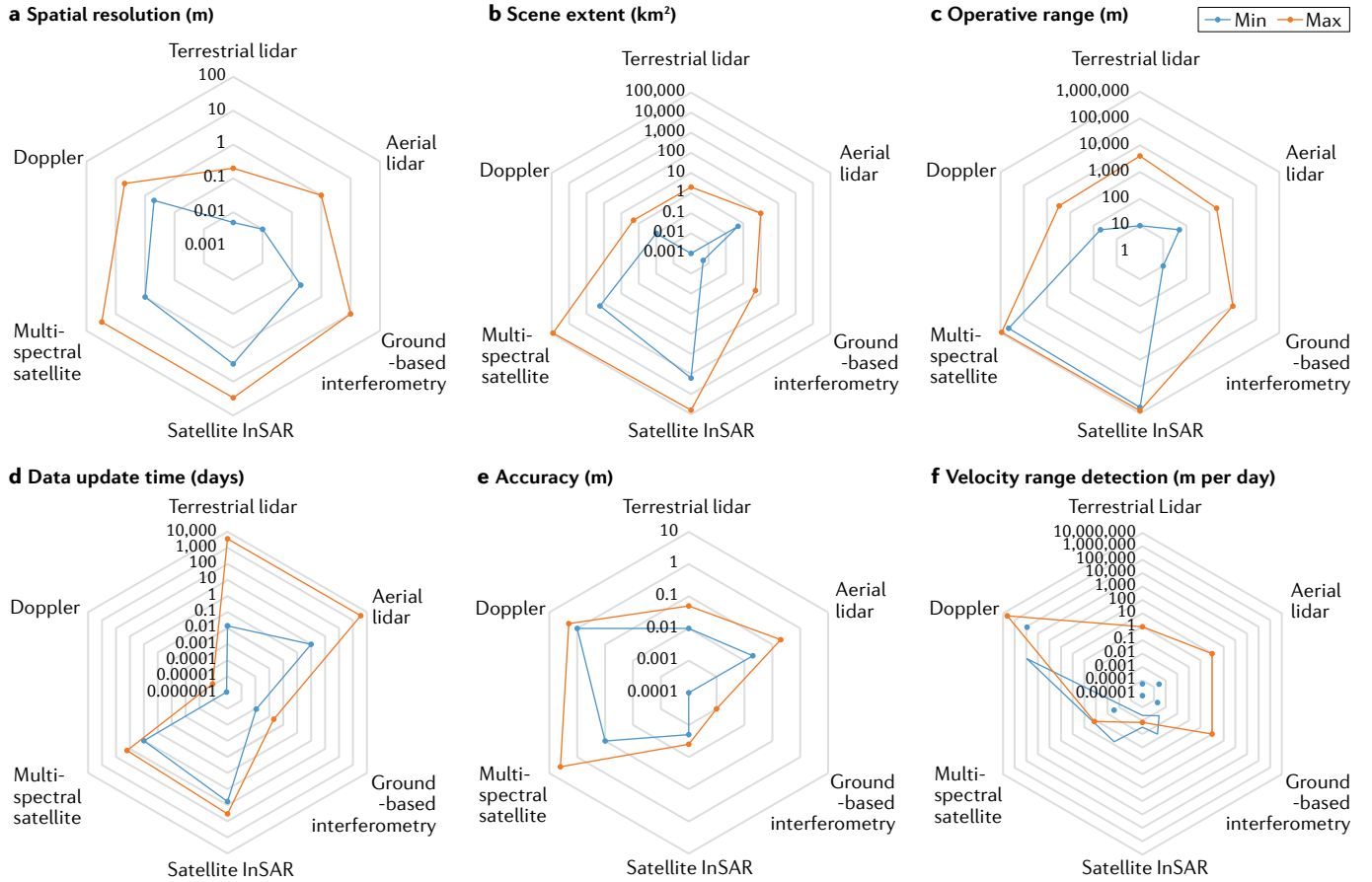

Fig. 2 | Technical comparison between different remote-sensing techniques. Every described technique has a range of operability. **a**, Spatial resolution. **b**, Extent of the area that can be surveyed. **c**, Distance from the target. **d**, Frequency of the acquisitions. **e**, Accuracy. **f**, Velocity of the target. Each technique has its own strong and weak points, which means that none is suitable for every application and type of landslide. InSAR, interferometric synthetic aperture radar.

Owing to the wide spatial coverage and cost–effectiveness, satellite applications (both radar and multispectral-based) are suitable in scanning wide areas and spotting localized deformations, especially in hazardous zones in which field activities can be challenging or unfeasible. Existing satellite SAR and multispectral sensors are theoretically appropriate for landslide detection and mapping in a wide range of settings in terms of wavelength, ground resolution and temporal repetitiveness. Rather than relying on a single sensor, the adoption of different spectral intervals (visible, infrared, C-band, X-band and L-band) is encouraged, as it mitigates intrinsic limitations of any one particular sensor. Moreover, the synergic use of different techniques can extend observation capabilities, allowing for the detection and mapping of different deformation regimes; although slow-moving landslides can be analysed using both DInSAR and MTInSAR approaches, rapid landslides can be successfully detected only with interferograms, that is, from the comparison of just two acquisitions. In the case of very fast displacements (the maximum detectable velocity ranges from several centimetres to a few hundreds of centimetres, depending on wavelength and revisiting time of the sensor), reliable information on surface displacement can be obtained using only approaches based on multispectral change detection and amplitude tracking.

Ground-based techniques are also increasingly helpful in landslide detection. At the local scale, high accuracy and flexibility make ground-based techniques extremely useful to retrieve basic information regarding the rate and the extent of deformation of single (or a group of) landslide (or landslides). Ground-based interferometry, for example, can be used for rapid mapping by performing 2D acquisitions to cover areas beyond those that were initially considered of interest and potentially to detect further unstable portions of a slope.

Lidar is widely used in landslide characterization and detection[93]. For example, the visual inspection of high-resolution digital elevation models provided by lidar often greatly improves landslide mapping capabilities[94,95] as interesting features, such as fractures, strata, debris deposits, overhanging rocks and so on, can be recognized on a 3D reconstruction. The high resolution of point clouds acquired by terrestrial lidars allows for a complete geomechanical characterization of rock masses, especially in demanding environments[96–98]. Finally, the comparison of two point clouds taken at different times allows for landslide volume estimation and identification of rockfall source areas[99,100].

Monitoring

Following its identification, it is fundamental to measure the key parameters of a landslide, most notably its surface displacement over time. Multispectral images are suitable in monitoring landslide motion[101],

Glossary

Interferometry
A technique that calculates the displacement of a target by measuring the phase shift between two electromagnetic waves that have been backscattered by the same target in two different times.

Multispectral
The range of the electromagnetic spectrum from 0.4 µm to about 12.5 µm.

Multispectral band
A specific wavelength range across the electromagnetic spectrum that roughly corresponds to the blue, green and red visible light up to near and shortwave infrared that are captured by multispectral sensors.

Radar
A sensor that emits signals within specific bands of the microwave domain, corresponding to different wavelengths.

Revisiting time
The time interval between two consecutive observations of an area.

Synthetic aperture radar
A technique that moves the antennas of a radar interferometer to obtain data with a spatial resolution equal to that of a sensor with antennas as large as the entire trajectory length.

despite obvious limitations related to cloud cover and, until late 1990s, to insufficient spatial resolution[6]. Effectiveness of multispectral imaging monitoring increased with the advent of VHR satellite imagery (IKONOS and QuickBird) and with the launch of the Sentinel-2 mission[102], which provides regular and frequent acquisitions with global coverage.

Image correlation can be used to quantify landslide evolution[103,104]. This method uses moving windows to calculate the correlation between texture similarities in pairs of diachronic images and is the most popular and effective method to derive sub-pixel displacements, for example, using aerial photographs and QuickBird satellite images[105], Pléiades satellites[106] or Landsat-8 acquisitions[107] on different types of landslide. Slope displacement time series using Sentinel-2 images[108] or the SPOT1 and SPOT5–Pléiades archive[109] have also been obtained. Other than landslide kinematics, successive retrogressive and advancing phases can be successfully reconstructed[110] as well, with short revisiting time satellites.

There are methods to detect and monitor slow-moving landslides (ranging from millimetres per day to few centimetres per day[111]), but most image correlation methods are only suitable for monitoring landslides moving at metre-to-decametre rates per year. These methods tend to have an accuracy between one-eighth and one-half of a pixel size, depending on the sensor[106], with Pléiades providing the lowest uncertainties[112]. The availability of large, continuous image datasets reduces the uncertainty, as full data redundancy contributes to creating a more robust time series of displacement[109]. Moreover, for a given reference image, using images acquired during a similar time of the year further reduces displacement uncertainties[108] related to the conditions of acquisition and background noise. Different satellite sources with similar spectral and spatial properties (Landsat-7, Landsat-8 and Sentinel-2) can be combined to create dense time series[113].

Concerning satellite SAR, displacement time series are the most advanced product of any multitemporal interferometric processing and provide the temporal pattern of deformation of each MP for each acquisition over the observed period. When supported by other instrumentation and field surveys, visual[114], semi-automatic[115] and automatic analysis[116] of time series can support the characterization and monitoring of landslide kinematics[117], zonation of sectors[118], the identification of post-seismic[119] and rainfall-induced[120] velocity changes, seasonal variations[121] and the monitoring of remedial works performance[122]. Furthermore, the shorter than a week revisiting time of satellites such as Sentinel-1, TerraSAR-X or COSMO-SkyMed makes landslide monitoring at the regional scale feasible with a systematic regularity[123].

Although satellite interferometry is clearly useful, interferometric landslide monitoring requires the presence of suitable targets in the area to be imaged by the radar sensors, such as buildings and artificial objects, which can provide good phase stability for interferometric applications; conversely, the response from bare soil, crops and vegetated areas can be insufficient or even non-existent in non-urban areas. Artificial targets[124], in the form of active and passive corner reflectors[125], can be used for both deformation monitoring studies in crops and bare soil areas[126] and accuracy assessment of InSAR measurements[127].

Although interferometric landslide monitoring works well for slower landslide rates, ground-based radar interferometry has near real-time acquisition frequency and so is able to measure movement rates up to several metres per day[128]. Therefore, this technique is suitable for monitoring most landslides during the phases preceding the possible catastrophic failure, such as earth flows[17], earth slides[16], large rockslides[129] and unstable volcanic flanks[130]. Very or extremely rapid movements (Box 1) such as rockfalls are too fast to be measured with radar interferometry, but can be successfully monitored by Doppler radar, which can also be coupled with early warning systems, for example, to close endangered streets (Fig. 3).

Like radar-based monitoring, multitemporal lidar surveys can be used to monitor different types of landslide processes. The introduction of automated terrestrial laser scanners has increased the data acquisition frequency. However, automatic data processing is required, especially for early warning applications[131], limiting its current application for monitoring.

Overall, satellite methods are suitable for systematic tracking of ground deformation phenomena at the regional scale. Accurate, high-frequency data from sensors installed in situ enable the understanding of specific details of the deformative process and, eventually, the identification of precursory signs leading to landslide failure.

Table 1 | Suitability of the techniques for the most common types of landslides

Technique	Detection	Monitoring	Prediction (time of failure)
MTInSAR	ES, RS, EF, LS, SL[a]	ES, RS, EF, LS, SL[a]	ES[a], RS[a]
Multispectral satellite sensors	ES, RS, EF, LS, SL[a], DF	ES, RS, EF, LS, SL[a]	ES, RS, EF[a]
Ground-based interferometry	ES, RS, LS	ES, RS, EF, LS[a], SL[a]	ES, RS, EF[a]
Doppler radar	RF	RF, DF, SL	—
Lidar	ES, RS, EF, LS, RF	ES, RS, EF, LS	—

For each landslide type, a typical velocity is assumed as follows: earth slide (ES; from <1.6 m per year to 1.8 m h^{-1}), rockslide (RS; from <1.6 m per year to >1.8 m h^{-1}), rockfall (RF; >1.8 m h^{-1}), earth flow (EF; from 1.6 m per year to 1.8 m h^{-1}), debris flow (DF; >1.8 m h^{-1}), lateral spread (LS; from <1.6 m per year to 1.8 m h^{-1}) and shallow landslide (SL; from <1.6 m per year to >1.8 m h^{-1}). MTInSAR, multitemporal interferometric synthetic aperture radar. [a]The applicability is limited.

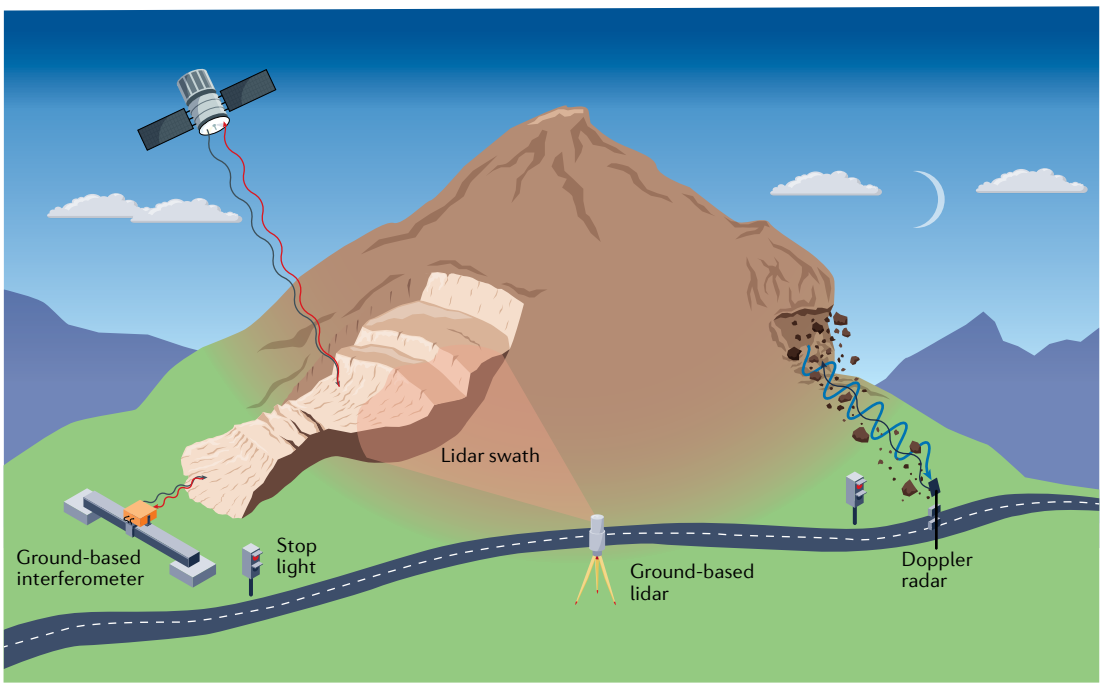

Fig. 3 | Site monitoring with remote-sensing techniques. Lidar, satellite and ground-based interferometry can be used to monitor slower landslides (left side of the hill), and Doppler radar is used for fast or extremely fast movements such as rockfalls (right side of the hill). The traffic lights next to the ground-based interferometer and Doppler radar indicate the use of near real-time measurements to provide early warnings.

Prediction

The ultimate goal of landslide monitoring is prediction (or forecast): the ability to timely, accurately and efficiently estimate one (or more) parameters connected to the future failure of a landslide[132]. Failure usually means a catastrophic evolution of the landslide, leading to a strong increase in velocity and runout[132], often associated with a total or partial disintegration of the material involved and formation of macrocracks. The precise requirements for timeliness, accuracy and efficiency vary from case to case, as they depend on the scale of the forecast (large areas require longer lead time), the type of elements at risk (people, critical infrastructures and cultural heritage), the type of countermeasures needed (town evacuations, street closures and clearance of a sector of an open-pit mine) and the level of preparation of the people responding to the prediction, for example.

The prediction of the time of failure (ToF) of a landslide relies on ground displacement data (or the derivative velocity and acceleration), rainfall amount or, less commonly, variables such as acoustic or seismic emissions related to progressive fracturing[133]. Of these three approaches, ground displacement data are the most widely used at the slope scale[134–137] because displacement represents a direct measurement of the stability conditions. However, rainfall is preferred when forecasting at the regional scale, in which diffused and near real-time displacement measurements are typically not available. Predictions based on other parameters, all measurable at the slope scale only, are less common as it is more difficult to relate to the possible collapse.

The general assumption behind ToF forecasting based on displacement is that the final rupture is typically preceded by a power-law acceleration called tertiary creep, which can be modelled to extrapolate the time of collapse. For this reason, almost all the ToF prediction methods only rely on displacement data acquired during the tertiary creep stage[138–140] (Box 2).

The advance with which predictions are possible generally depends on the size of the landslide and on the type of the material. Landslides on the scale of millions of cubic metres can display early signs of tertiary creep tens of days before the collapse[141,142], allowing for a practically feasible prediction 1 week or more before the failure. Stiff and brittle rocks tend to collapse abruptly[143], limiting warning time, although rapidly measuring instruments such as GBInSAR are now able to provide a few hours of lead time, even for smaller slides of a few tens of thousands of cubic metres[144]. The failure mechanism also seems to affect the predictability of a landslide – masses in which a sliding surface is developing through the propagation of an underground crack tend to respond well to tertiary creep modelling[145]. However, the interference of external factors (such as human activities) and complex geological conditions makes it impossible to be conclusive on a precise relation between failure mechanism and failure prediction.

The ability of an instrument to monitor versus to forecast is determined by whether it can make new acquisitions (and the necessary elaborations) at a frequency compatible with the evolution of the landslide. A high acquisition rate serves to follow every step of the kinematic evolution of a landslide, particularly its accelerations, to model what could come next, especially when a paroxysmal collapse can occur (ToF prediction in strict sense). However, even without a proper prediction model capable of providing a date or an hour of probable collapse, the incoming collapse can become evident by a strong increase (sometimes tenfold or higher) in the displacement velocity, so a high acquisition frequency is important also to issue a warning based on some apparent mobilization or empirical threshold.

Nevertheless, a prediction approach based on models — even empirical models — generally requires some data elaborations not compatible with all landslide velocities. For example, the Doppler radar is proficient at early warning against rockfalls and debris flows, as it gives a signal as these very or extremely rapid landslides have already started to catastrophically move down the slope. By contrast, ground-based interferometry is more suitable for ToF prediction; considering the time needed to process and interpret data, a delay of tens of minutes is possible before an alert can be issued. Nevertheless, this lead time can still be considered a very good early warning performance for those landslides that experience slow or moderate velocity during the tertiary creep (such as rockslides, rock avalanches, deep-seated earth slides or particularly large rockfalls; Box 2). Moreover, when the movement rates of these landslides increase shortly before collapsing, a ToF prediction can already been made during the preceding acceleration phase (Fig. 4).

Ground-based techniques are the most widely used in landslide prediction, but the launch of the Sentinel-1 twin satellites[146] has enhanced the use of InSAR in the landslide analysis and presents new possibilities for failure forecast. In particular, these satellites provide a relatively short revisiting time (a 6-day repeat cycle in Europe and some other areas, globally 12 days), regional-scale mapping capability (because of the large 250-km swath) and a systematic and regular acquisition plan. Post-events analyses on a large catastrophic rockslide in China have shown a clear acceleration weeks before the failure, which could have enabled an accurate ToF prediction and to prevent many human losses[142,147].

Satellite multispectral data, systematically acquired over large areas with short revisiting time, also could be useful for large landslide prediction and warning, at least for some typologies of sliding phenomena. For example, a 9-month time series of displacement for a landslide in the French Alps was observed using the 5-day revisiting time of the Sentinel-2 satellites, capturing a sudden reactivation leading to a failure[109]. Similarly, a large Sentinel-2 archive and a pixel off-track method were exploited to derive possible precursors before a landslide in the southern Himalayas[148].

Box 2

Successful landslide monitoring and forecasting

Gallivaggio Sanctuary (near Chiavenna, Italy) is a cultural heritage site that was threatened by an unstable rock mass hanging from a 500-m high, sub-vertical granitic wall. A ground-based interferometric synthetic aperture radar (GBInSAR) was installed in 2016, which detected a 5,000 m^3 rock mass experiencing continuous deformation and threatening both the sanctuary and the nearby road[164]. Traffic and access to the sanctuary were regulated by a sequence of alert thresholds, and restrictive orders were issued according to the measured velocities. On 29 May 2019, the rock mass collapsed, as shown in a frame from a 29 May 2018 footage recording the failure of the landslide (see the figure), and left a 15-m wide scar on the rock mass[164]. The time of failure was accurately predicted several hours in advance, so despite damage to both the road and the buildings, the timely evacuation of the area prevented any loss of life.

An early warning system based on displacement velocity thresholds was also implemented in Veslemannen, Norway, which comprised colour-coded hazard levels (green, yellow, orange and red, with red implying evacuation). The monitoring included GBInSAR, a network of extensometers, and time-lapse cameras, observing a 54,000 m^3 active portion of the larger Mannen unstable rock slope[152]. The landslide experienced a gradual acceleration over the years, triggering as many as 16 evacuations from 2014 to 2019, including the last one before the actual slope failure. The last warning was accompanied by displacement velocities high enough to be at the limits of GBInSAR capabilities and eventually, 1h before the collapse, a complete loss of coherence occurred in the GBInSAR data. Continuous and transparent communication with local population and authorities was crucial to public trust in the warning system, which effectively prevented any human loss.

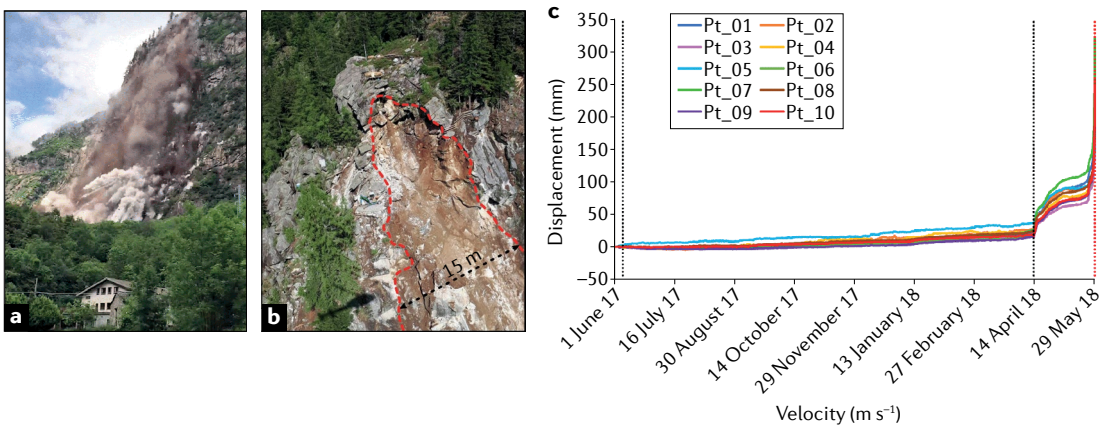

The figure is adapted from ref.[164], CC BY 4.0 (https://creativecommons.org/licenses/by/4.0/).

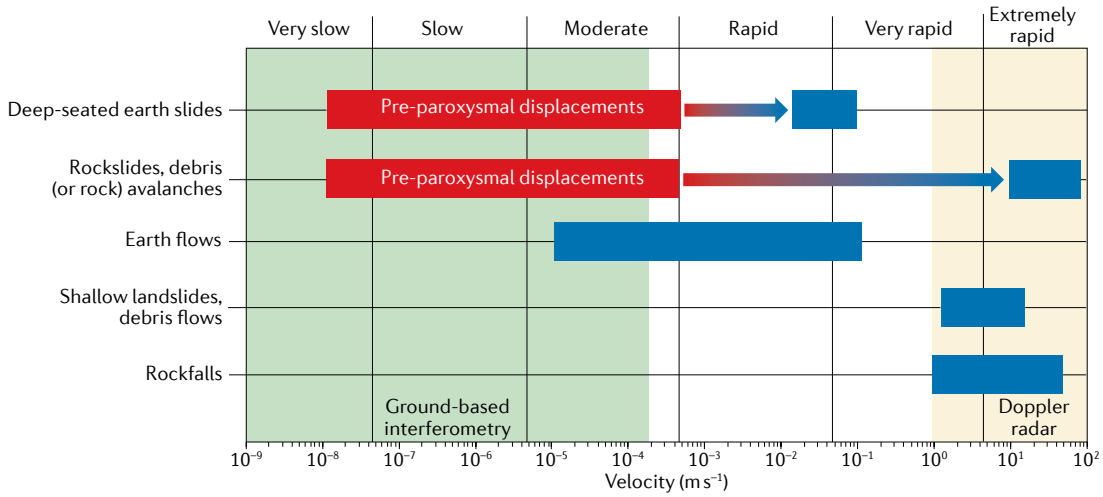

Fig. 4 | The field of action of ground-based interferometry and Doppler radar in common types of landslides. The green and yellow areas show the velocity range within which ground-based interferometry and Doppler radar can operate, respectively. Some types of landslides, such as rockslides and deep-seated earth slides, can experience sudden exponential accelerations (represented by the arrows transitioning from red to blue) just days or hours before failure, thus exhibiting movement rates beyond ground-based interferometric capabilities; however, the trend measured during the pre-paroxysmal phase (in red) can be enough to extrapolate the prediction of the time of failure.

Summary and future perspectives

Remote sensing is critical in the detection, monitoring and prediction of landslides. New and improved technologies now collect an array of information on different types of slope instabilities at multiple scales. In general, owing to new algorithms, and sensors with a higher acquisition frequency and spatial resolution, we are now able to monitor fast landslides that were beyond instrumental capabilities until the late 2010s and to better detect and contour slope instabilities in remote and vegetated areas.

The current bottleneck in landslide monitoring and prediction is not only the ability to collect landslide data but also to fully exploit it. For example, satellites continuously acquire and archive images that could detect, monitor and, in some cases, predict people-threatening landslides, but that are often analysed only after catastrophic events[142]. Ground-based interferometry produces displacement maps consisting of thousands of pixels; however, the common practice is to arbitrarily select only a few control points instead of using the full spatial coverage provided by the radar[149]. A partial solution to these data underexploitation could be a more open sharing policy within the scientific community and in a more intense exchange among industry, local administrators and researchers. In general, the more that data circulate, the more likely they will be used.

In addition to better exploiting existing data, the geographical scope of landslide monitoring must expand. Additional research and monitoring are needed in developing areas where population and/or landslide susceptibility are expected to increase and in low-income countries that might have less capability to adopt prevention policies to mitigate landslide impact. The European Ground Motion Service by Copernicus Land Monitoring Service[150], whose first baseline release was in mid-2022 and is the largest wide-area MTInSAR deformation monitoring system, is an example of broad-scale monitoring. On the basis of Sentinel-1 SAR data processed at full resolution, the European Ground Motion Service provides free seamless information regarding natural and anthropogenic ground motion phenomena over Europe, fundamental for landslide mapping and monitoring, including less investigated areas. In the near future, these ground displacement data will increase the need for algorithms capable of spotting prone-to-failure areas.

The integration of different techniques should be a focus of landslide science in the next 5–10 years. With the launch planned for January 2023, the NISAR mission will be the first dual-frequency fully polarimetric SAR satellite, operating in both L and S (3.2 GHz, ~9.3 cm wavelength) microwave bands[151]. Integration of data from multiple bands will provide deeper insight into the dynamics of landslides, especially in vegetated areas[72]. Displacement maps produced by ground-based interferometers bear with them geometrical distortions that make them difficult to interpret without projecting them over a georeferenced map or a 3D reconstruction of the environment. Today, these projection procedures are standard post-processing (Fig. 1e) but require time and effort. Therefore, the next generation of ground-based interferometers should include an integrated laser scanner to directly produce 3D images of the scenario displaying the point-by-point displacement; the comparison of multiple laser scans could also enable to correct noisy interferometric measurements and to encompass larger displacement rates without the limitation of the LOS. Similarly, Doppler and ground-based interferometry should be integrated in a single tool capable of covering a large range (around 10 orders of magnitude) of landslide velocities (Fig. 4).

However, in landslide monitoring and management, it is also critical that there is an appropriate match between the cost of instrumenting an area and its actual use. For instance, when an integrated and expensive monitoring network is set into place to deal with a large landslide that has recently shown signs of reactivation, the high cost could reduce the length of time when this system can be kept working owing to long maintenance cost. Using less costly instruments for a long-term monitoring campaign on one or more landslides could ultimately increase the probability that any resulting collapse is monitored.

To increase the efficacy of these systems, we recommend that forecasting methods based on tertiary creep be incorporated in early warning systems. They currently are not, mostly owing to noise and to the difficulty in discriminating normal acceleration phases from the final acceleration preceding the catastrophic collapse (as exemplified in Box 2 (ref.[152])). However, moments preceding failure are ultimately clearly distinguishable from other (seasonal) reactivations, as the episode leading to failure usually reaches higher velocity and acceleration values[153]. Formalizing these differences to increase the confidence and the advance necessary to discriminate false alarms from true alarms during emergencies is a much-needed step forward for decision-makers.

Finally, landslide management incorporates technological and social aspects, so risk communication and perception are clearly important. Good communication strategies[154,155] and technologically advanced monitoring and early warning systems are not always paired in practice, so even the most accurate predictions made with advanced RSTs will not be effective if the warnings do not reach the population. Raising risk awareness is a cost-effective means to reduce risk by diminishing the exposure to a hazard with unsafe behaviours and increasing the understandability and efficacy of landslide warnings[156].

Published online: 10 January 2023

References

1. Bennett, G. L., Miller, S. R., Roering, J. J. & Schmidt, D. A. Landslides, threshold slopes, and the survival of relict terrain in the wake of the Mendocino Triple Junction. *Geology* **44**, 363–366 (2016).
2. Moreiras, S. M. Climatic effect of ENSO associated with landslide occurrence in the Central Andes, Mendoza Province, Argentina. *Landslides* **2**, 53–59 (2005).
3. Petley, D. N. et al. Trends in landslide occurrence in Nepal. *Nat. Hazards* **43**, 23–44 (2007).
4. Froude, M. J. & Petley, D. N. Global fatal landslide occurrence from 2004 to 2016. *Nat. Hazards Earth Syst. Sci.* **18**, 2161–2181 (2018).
5. Patton, A. I., Rathburn, S. L. & Capps, D. M. Landslide response to climate change in permafrost regions. *Geomorphology* **340**, 116–128 (2019).
6. Mantovani, F., Soeters, R. & Van Westen, C. J. Remote sensing techniques for landslide studies and hazard zonation in Europe. *Geomorphology* **15**, 213–225 (1996).
7. Metternicht, G., Hurni, L. & Gogu, R. Remote sensing of landslides: an analysis of the potential contribution to geo-spatial systems for hazard assessment in mountainous environments. *Remote Sens. Environ.* **98**, 284–303 (2005).
8. Delacourt, C. et al. Remote-sensing techniques for analysing landslide kinematics: a review. *Bull. Soc. Géol. Fr.* **178**, 89–100 (2007).
9. Crosetto, M., Monserrat, O., Cuevas-González, M., Devanthéry, N. & Crippa, B. Persistent scatterer interferometry: a review. *ISPRS J. Photogramm. Remote Sens.* **115**, 78–89 (2016).
10. Mondini, A. C. et al. Landslide failures detection and mapping using synthetic aperture radar: past, present and future. *Earth Sci. Rev.* **216**, 103574 (2021).
11. Casagli, N. et al. Spaceborne, UAV and ground-based remote sensing techniques for landslide mapping, monitoring and early warning. *Geoenviron. Disasters* **4**, 9 (2017).
12. Lillesand, T., Kiefer, R. W. & Chipman, J. *Remote Sensing and Image Interpretation* (John Wiley & Sons, 2014).
13. Jaboyedoff, M. et al. Use of LIDAR in landslide investigations: a review. *Nat. Hazards* **61**, 5–28 (2012).
14. Salvini, R., Francioni, M., Riccucci, S., Bonciani, F. & Callegari, I. Photogrammetry and laser scanning for analyzing slope stability and rock fall runout along the Domodossola–Iselle railway, the Italian Alps. *Geomorphology* **185**, 110–122 (2013).
15. Rosi, A. et al. The new landslide inventory of Tuscany (Italy) updated with PS-InSAR: geomorphological features and landslide distribution. *Landslides* **15**, 5–19 (2018).
16. Lombardi, L. et al. The Calatabiano landslide (southern Italy): preliminary GB-InSAR monitoring data and remote 3D mapping. *Landslides* **14**, 685–696 (2017).
17. Ferrigno, F., Gigli, G., Fanti, R., Intrieri, E. & Casagli, N. GB-InSAR monitoring and observational method for landslide emergency management: the Montaguto earthflow (AV, Italy). *Nat. Hazards Earth Syst. Sci.* **17**, 845–860 (2017).
18. Intrieri, E. et al. Big data managing in a landslide early warning system: experience from a ground-based interferometric radar application. *Nat. Hazards Earth Syst. Sci.* **17**, 1713–1723 (2017).
19. MacDonald, H. C. & Grubbs, R. S. *NASA Lyndon B. Johnson Space Center NASA Earth Resources Survey Symposium* Vol. 1-B (NASA, 1975).
20. Zhao, C. & Lu, Z. Remote sensing of landslides: a review. *Remote Sens.* **10**, 279 (2018).
21. Martha, T. R., Kerle, N., Van Westen, C. J., Jetten, V. & Kumar, K. V. Object-oriented analysis of multi-temporal panchromatic images for creation of historical landslide inventories. *ISPRS J. Photogramm. Remote Sens.* **67**, 105–119 (2011).
22. Hölbling, D. et al. Comparing manual and semi-automated landslide mapping based on optical satellite images from different sensors. *Geosciences* **7**, 37 (2017).
23. Solari, L. et al. Review of satellite interferometry for landslide detection in Italy. *Remote Sens.* **12**, 1351 (2020).
24. Guzzetti, F. et al. Landslide inventory maps: new tools for an old problem. *Earth Sci. Rev.* **112**, 42–66 (2012).
25. Scaioni, M., Longoni, L., Melillo, V. & Papini, M. Remote sensing for landslide investigations: an overview of recent achievements and perspectives. *Remote Sens.* **6**, 9600–9652 (2014).
26. Tofani, V., Segoni, S., Agostini, A., Catani, F. & Casagli, N. Technical note: use of remote sensing for landslide studies in Europe. *Nat. Hazards Earth Syst. Sci.* **13**, 299–309 (2013).
27. Savvaidis, P. D. Existing landslide monitoring systems and techniques. In *From Stars to Earth and Culture* 242–258 (Academia, 2003).
28. Ose, K., Corpetti, T. & Demagistri, L. in *Optical Remote Sensing of Land Surface* 57–124 (Elsevier, 2016).
29. Li, J. & Roy, D. P. A global analysis of Sentinel-2A, Sentinel-2B and Landsat-8 data revisit intervals and implications for terrestrial monitoring. *Remote. Sens.* **9**, 902 (2017).
30. Li, J. & Chen, B. Global revisit interval analysis of Landsat-8-9 and Sentinel-2A-2B data for terrestrial monitoring. *Sensors* **20**, 6631 (2020).
31. Jacobsen, K. *Characteristics of very high resolution optical satellites for topographic mapping* (isprs, 2011); https://www.int-arch-photogramm-remote-sens-spatial-inf-sci.net/XXXVIII-4-W19/137/2011/.
32. Li, S., Kang, X., Fang, L., Hu, J. & Yin, H. Pixel-level image fusion: a survey of the state of the art. *Inf. Fusion* **33**, 100–112 (2017).
33. Santurri, L. et al. Assessment of very high resolution satellite data fusion techniques for landslide recognition. In *ISPRS TC VII Symposium– 100 Years Vienna, Austria* (eds Wagner, W. & Székely, B.) 5–7 (ISPRS, 2010).
34. Curlander, J. C. & McDonough, R. N. *Synthetic Aperture Radar* Vol. 11 (Wiley, 1991).
35. Wasowski, J. & Bovenga, F. Investigating landslides and unstable slopes with satellite multi temporal interferometry: current issues and future perspectives. *Eng. Geol.* **174**, 103–138 (2014).
36. Bamler, R. & Hartl, P. Synthetic aperture radar interferometry. *Inverse Probl.* **14**, R1 (1998).
37. Gabriel, A. K., Goldstein, R. M. & Zebker, H. A. Mapping small elevation changes over large areas: differential radar interferometry. *J. Geophys. Res. Solid Earth* **94**, 9183–9191 (1989).
38. Massonnet, D. & Feigl, K. L. Discrimination of geophysical phenomena in satellite radar interferograms. *Geophys. Res. Lett.* **22**, 1537–1540 (1995).
39. Zebker, H. A. & Villasenor, J. Decorrelation in interferometric radar echoes. *IEEE Trans. Geosci. Remote Sens.* **30**, 950–959 (1992).
40. Ferretti, A., Prati, C. & Rocca, F. Permanent scatterers in SAR interferometry. *IEEE Trans. Geosci. Remote Sens.* **39**, 8–20 (2001).
41. Berardino, P., Fornaro, G., Lanari, R. & Sansosti, E. A new algorithm for surface deformation monitoring based on small baseline differential SAR interferograms. *IEEE Trans. Geosci. Remote Sens.* **40**, 2375–2383 (2002).
42. Conforti, M., Pascale, S., Pepe, M., Sdao, F. & Sole, A. Denudation processes and landforms map of the Camastra River catchment (Basilicata–South Italy). *J. Maps* **9**, 444–455 (2013).
43. Zhou, X., Chang, N.-B. & Li, S. Applications of SAR interferometry in earth and environmental science research. *Sensors* **9**, 1876–1912 (2009).
44. Colesanti, C., Ferretti, A., Locatelli, R., Novali, F. & Savio, G. In *2003 IEEE International Geoscience and Remote Sensing Symposium Proceedings* 1193–1195 (IEEE, 2003).
45. Michel, R. M., Avouac, J. P. & Taboury, J. Measuring ground displacements from SAR amplitude images: application to the Landers earthquake. *Geophys. Res. Lett.* **26**, 875–878 (1999).
46. Strozzi, T., Luckman, A., Murray, T., Wegmuller, U. & Werner, C. L. Glacier motion estimation using SAR offset-tracking procedures. *IEEE Trans. Geosci. Remote Sens.* **40**, 2384–2391 (2002).
47. De Zan, F. Accuracy of incoherent speckle tracking for circular Gaussian signals. *IEEE Geosci. Remote Sens. Lett.* **11**, 264–267 (2014).
48. Reeves, B., Noon, D. A., Stickley, G. F. & Longstaff, D. Slope stability radar for monitoring mine walls. In *Proc. Subsurface and Surface Sensing Technologies and Applications III* Vol. (ed. Nguyen, C.) 57–67 (SPIE, 2001).
49. Tarchi, D. et al. SAR interferometry for structural changes detection: A demonstration test on a dam. In *IEEE 1999 International Geoscience and Remote Sensing Symposium* 1522–1524 (IEEE, 1999).
50. Atzeni, C. et al. Ground-based radar interferometry for landslide monitoring and control. In *Proc. ISSMGE Field Workshop on Landslides and Natural/Cultural Heritage Trabzon (Turkey)* 195–209 (ISSMGE, 2001).
51. Dick, G. J., Eberhardt, E., Cabrejo-Liévano, A. G., Stead, D. & Rose, N. D. Development of an early-warning time-of-failure analysis methodology for open-pit mine slopes utilizing ground-based slope stability radar monitoring data. *Can. Geotech. J.* **52**, 515–529 (2015).
52. Carlà, T., Farina, P., Intrieri, E., Ketizmen, H. & Casagli, N. Integration of ground-based radar and satellite InSAR data for the analysis of an unexpected slope failure in an open-pit mine. *Eng. Geol.* **235**, 39–52 (2018).
53. Di Traglia, F. et al. Ground-based InSAR reveals conduit pressurization pulses at Stromboli volcano. *Terra Nova* **25**, 192–198 (2013).
54. Del Ventisette, C. et al. Using ground based radar interferometry during emergency: the case of the A3 motorway (Calabria Region, Italy) threatened by a landslide. *Nat. Hazards Earth Syst. Sci.* **11**, 2483–2495 (2011).

55. Gubler, H. Five years experience with avalanche-, mudflow-, and rockfall-alarm systems in Switzerland. In *Proc. International Snow Science Workshop* 1–9 (ISSW, 2000).
56. Meier, L., Jacquemart, M., Blattmann, B. & Arnold, B. Real-time avalanche detection with long-range, wide-angle radars for road safety in Zermatt, Switzerland. In *Proc. International Snow Science Workshop* 304–308 (ISSW, 2016).
57. Cui, P., Guo, X., Yan, Y., Li, Y. & Ge, Y. Real-time observation of an active debris flow watershed in the Wenchuan Earthquake area. *Geomorphology* **321**, 153–166 (2018).
58. Mikoš, M. & Huebl, J. Practice guidelines on monitoring and warning technology for debris flows: TXT-tool 2.386-1.2. *Landslide Dyn. ISDR-ICL Landslide Interact. Teach. Tools* **1**, 567–585 (2018).
59. Meier, L., Jacquemart, M., Wahlen, S. & Blattmann, B. Real-time rockfall detection with doppler radars. In *Proc. 6th Interdisciplinary Workshop on Rockfall Protection* 1–4 (CIMNE, 2017).
60. Michelini, A. et al. A new radar-based system for detecting and tracking rockfall in open pit mines. In *Proc. 2020 International Symposium on Slope Stability in Open Pit Mining and Civil Engineering* 1183–1192 (Australian Centre for Geomechanics, 2020).
61. Wahlen, S. et al. Real-time rockfall detection system with automatic road closure and reopening using Doppler radar technology at the Ruinon Landslide, Italy. *EGU General Assembly 2021* https://doi.org/10.5194/egusphere-egu21-14818 (2021).
62. Viviani, F., Michelini, A. & Mayer, L. RockSpot: an Interferometric Doppler Radar for Rockfall/Avalanche Detection and Tracking. In *2020 IEEE Radar Conference* (*RadarConf20*) 1–5 (IEEE, 2020).
63. Mallet, C. M. & Bretar, F. D. R. Full-waveform topographic lidar: state-of-the-art. *ISPRS J. Photogramm. Remote Sens.* **64**, 1–16 (2009).
64. Brunsden, D. Mass movement: the research frontier and beyond: a geomorphological approach. *Geomorphology* **7**, 85–128 (1993).
65. Mondini, A. et al. Semi-automatic recognition and mapping of rainfall induced shallow landslides using optical satellite images. *Remote Sens. Environ.* **115**, 1743–1757 (2011).
66. Achache, J., Fruneau, B. & Delacourt, C. Applicability of SAR interferometry for monitoring of landslides. *ERS Appl.* **383**, 165 (1996).
67. Fruneau, B. N. D., Achache, J. & Delacourt, C. Observation and modelling of the Saint-Etienne-de-Tinée landslide using SAR interferometry. *Tectonophysics* **265**, 181–190 (1996).
68. Kimura, H. & Yamaguchi, Y. Detection of landslide areas using satellite radar interferometry. *Photogramm. Eng. Remote Sens.* **66**, 337–344 (2000).
69. Berardino, P. et al. Use of differential SAR interferometry in monitoring and modelling large slope instability at Maratea (Basilicata, Italy). *Eng. Geol.* **68**, 31–51 (2003).
70. Rott, H., Scheuchl, B., Siegel, A. & Grasemann, B. Monitoring very slow slope movements by means of SAR interferometry: a case study from a mass waste above a reservoir in the Ötztal Alps, Austria. *Geophys. Res. Lett.* **26**, 1629–1632 (1999).
71. Schlögel, R., Doubre, C., Malet, J.-P. & Masson, F. Landslide deformation monitoring with ALOS/PALSAR imagery: a D-InSAR geomorphological interpretation method. *Geomorphology* **231**, 314–330 (2015).
72. Bekaert, D. P. S., Handwerger, A. L., Agram, P. & Kirschbaum, D. B. InSAR-based detection method for mapping and monitoring slow-moving landslides in remote regions with steep and mountainous terrain: an application to Nepal. *Remote Sens. Environ.* **249**, 111983 (2020).
73. Singhroy, V., Alasset, P.-J., Couture, R. & Poncos, V. InSAR monitoring of landslides on permafrost terrain in Canada. In *2007 IEEE International Geoscience and Remote Sensing Symposium* 2451–2454 (IEEE, 2007).
74. Hao, J. et al. Investigation of a small landslide in the Qinghai-Tibet Plateau by InSAR and absolute deformation model. *Remote Sens.* **11**, 2126 (2019).
75. Yao, T. et al. Recent third pole's rapid warming accompanies cryospheric melt and water cycle intensification and interactions between monsoon and environment: multidisciplinary approach with observations, modeling, and analysis. *Bull. Am. Meteorol. Soc.* **100**, 423–444 (2019).
76. Cui, P. & Jia, Y. Mountain hazards in the Tibetan Plateau: research status and prospects. *Natl Sci. Rev.* **2**, 397–399 (2015).
77. Di Martire, D. et al. A nation-wide system for landslide mapping and risk management in Italy: the second Not-ordinary Plan of Environmental Remote Sensing. *Int. J. Appl. Earth Obs. Geoinf.* **63**, 143–157 (2017).
78. Meisina, C. et al. Geological interpretation of PSInSAR data at regional scale. *Sensors* **8**, 7469–7492 (2008).
79. Zhang, Y. et al. Detection of geohazards in the Bailong River Basin using synthetic aperture radar interferometry. *Landslides* **13**, 1273–1284 (2016).
80. Lauknes, T. et al. Detailed rockslide mapping in northern Norway with small baseline and persistent scatterer interferometric SAR time series methods. *Remote Sens. Environ.* **114**, 2097–2109 (2010).
81. Ciampalini, A. et al. Analysis of building deformation in landslide area using multisensor PSInSAR™ technique. *Int. J. Appl. Earth Obs. Geoinf.* **33**, 166–180 (2014).
82. Raspini, F. et al. The contribution of satellite SAR-derived displacement measurements in landslide risk management practices. *Nat. Hazards* **86**, 327–351 (2017).
83. Cigna, F., Bianchini, S. & Casagli, N. How to assess landslide activity and intensity with persistent scatterer interferometry (PSI): the PSI-based matrix approach. *Landslides* **10**, 267–283 (2013).
84. Tofani, V., Raspini, F., Catani, F. & Casagli, N. Persistent scatterer interferometry (PSI) technique for landslide characterization and monitoring. *Remote Sens.* **5**, 1045–1065 (2013).
85. Berti, M., Corsini, A., Franceschini, S. & Iannacone, J. Automated classification of persistent scatterers interferometry time series. *Nat. Hazards Earth Syst. Sci.* **13**, 1945–1958 (2013).
86. Cruden, D. M. & Varnes, D. J. in *Landslides: Investigation and Mitigation Special Report* 247 (eds Turner, A. K. & Schuster, R. L.) Ch. 3 (Transportation Research Board, National Academy of Sciences, 1996).
87. Strozzi, T. et al. Survey and monitoring of landslide displacements by means of L-band satellite SAR interferometry. *Landslides* **2**, 193–201 (2005).
88. Dong, J. et al. Mapping landslide surface displacements with time series SAR interferometry by combining persistent and distributed scatterers: a case study of Jiaju landslide in Danba, China. *Remote Sens. Environ.* **205**, 180–198 (2018).
89. Cignetti, M. et al. Taking advantage of the ESA G-pod service to study ground deformation processes in high mountain areas: a Valle d'Aosta case study, northern Italy. *Remote Sens.* **8**, 852 (2016).
90. Manconi, A. et al. Brief communication: rapid mapping of landslide events: the 3 December 2013 Montescaglioso landslide, Italy. *Nat. Hazards Earth Syst. Sci.* **14**, 1835–1841 (2014).
91. Raspini, F. et al. Exploitation of amplitude and phase of satellite SAR images for landslide mapping: the case of Montescaglioso (South Italy). *Remote Sens.* **7**, 14576–14596 (2015).
92. Singleton, A., Li, Z., Hoey, T. & Muller, J. P. Evaluating sub-pixel offset techniques as an alternative to D-InSAR for monitoring episodic landslide movements in vegetated terrain. *Remote Sens. Environ.* **147**, 133–144 (2014).
93. Jaboyedoff, M. & Derron, M.-H. in *Developments in Earth Surface Processes* Vol. 23 (Elsevier, 2020).
94. Ardizzone, F., Cardinali, M., Galli, M., Guzzetti, F. & Reichenbach, P. Identification and mapping of recent rainfall-induced landslides using elevation data collected by airborne Lidar. *Nat. Hazards Earth Syst. Sci.* **7**, 637–650 (2007).
95. Chigira, M., Tsou, C.-Y., Matsushi, Y., Hiraishi, N. & Matsuzawa, M. Topographic precursors and geological structures of deep-seated catastrophic landslides caused by Typhoon Talas. *Geomorphology* **201**, 479–493 (2013).
96. Sturzenegger, M. & Stead, D. Quantifying discontinuity orientation and persistence on high mountain rock slopes and large landslides using terrestrial remote sensing techniques. *Nat. Hazards Earth Syst. Sci.* **9**, 267–287 (2009).
97. Gigli, G. & Casagli, N. Semi-automatic extraction of rock mass structural data from high resolution LIDAR point clouds. *Int. J. Rock Mech. Min. Sci.* **48**, 187–198 (2011).
98. Battulwar, R., Zare-Naghadehi, M., Emami, E. & Sattarvand, J. A state-of-the-art review of automated extraction of rock mass discontinuity characteristics using three-dimensional surface models. *J. Rock Mech. Geotech. Eng.* **13**, 920–936 (2021).
99. Giordan, D. et al. Morphological and kinematic evolution of a large earthflow: the Montaguto landslide, southern Italy. *Geomorphology* **187**, 61–79 (2013).
100. Frodella, W. et al. Synergic use of satellite and ground based remote sensing methods for monitoring the San Leo rock cliff (northern Italy). *Geomorphology* **264**, 80–94 (2016).
101. Hervás, J. et al. Monitoring landslides from optical remotely sensed imagery: the case history of Tessina landslide, Italy. *Geomorphology* **54**, 63–75 (2003).
102. Drusch, M. et al. Sentinel-2: ESA's optical high-resolution mission for GMES operational services. *Remote Sens. Environ.* **120**, 25–36 (2021).
103. Leprince, S., Barbot, S., Ayoub, F. & Avouac, J.-P. Automatic and precise orthorectification, coregistration, and subpixel correlation of satellite images, application to ground deformation measurements. *IEEE Trans. Geosci. Remote Sens.* **45**, 1529–1558 (2007).
104. Leprince, S. B., Berthier, E., Ayoub, F. O., Delacourt, C. & Avouac, J. P. Monitoring earth surface dynamics with optical imagery. *Eos Trans. Am. Geophys. Union* **89**, 1–2 (2008).
105. Delacourt, C., Allemand, P., Casson, B. & Vadon, H. Velocity field of the 'La Clapière' landslide measured by the correlation of aerial and QuickBird satellite images. *Geophys. Res. Lett.* **31**, 2004GL020193 (2004).
106. Lacroix, P., Berthier, E. & Maquerhua, E. T. Earthquake-driven acceleration of slow-moving landslides in the Colca valley, Peru, detected from Pléiades images. *Remote Sens. Environ.* **165**, 148–158 (2015).
107. Xiong, Z. et al. Pre- and post-failure spatial–temporal deformation pattern of the Baige landslide retrieved from multiple radar and optical satellite images. *Eng. Geol.* **279**, 105880 (2020).
108. Yang, W. Selecting the best image pairs to measure slope deformation. *Sensors* **20**, 4721 (2020).
109. Bontemps, N., Lacroix, P. & Doin, M.-P. Inversion of deformation fields time-series from optical images, and application to the long term kinematics of slow-moving landslides in Peru. *Remote Sens. Environ.* **210**, 144–158 (2018).
110. Lacroix, P., Araujo, G., Hollingsworth, J. & Taipe, E. Self-entrainment motion of a slow-moving landslide inferred from Landsat-8 time series. *J. Geophys. Res. Earth Surf.* **124**, 1201–1216 (2019).
111. Stumpf, A., Malet, J.-P. & Delacourt, C. Correlation of satellite image time-series for the detection and monitoring of slow-moving landslides. *Remote Sens. Environ.* **189**, 40–55 (2017).
112. Stumpf, A., Malet, J. P., Allemand, P. & Ulrich, P. Surface reconstruction and landslide displacement measurements with Plèiades satellite images. *ISPRS J. Photogramm. Remote Sens.* **95**, 1–12 (2014).
113. Stumpf, A., Michéa, D. & Malet, J.-P. Improved co-registration of Sentinel-2 and Landsat-8 imagery for Earth surface motion measurements. *Remote Sens.* **10**, 160 (2018).

114. Cigna, F., Del Ventisette, C., Liguori, V. & Casagli, N. Advanced radar-interpretation of InSAR time series for mapping and characterization of geological processes. *Nat. Hazards Earth Syst. Sci.* **11**, 865–881 (2011).
115. Cigna, F., Tapete, D. & Casagli, N. Semi-automated extraction of deviation indexes (DI) from satellite persistent scatterers time series: tests on sedimentary volcanism and tectonically-induced motions. *Nonlinear Process. Geophys.* **19**, 643–655 (2012).
116. Hussain, E., Novellino, A., Jordan, C. & Bateson, L. Offline-online change detection for Sentinel-1 InSAR time series. *Remote Sens.* **13**, 1656 (2021).
117. Mateos, R. M. et al. The combined use of PSInSAR and UAV photogrammetry techniques for the analysis of the kinematics of a coastal landslide affecting an urban area (SE Spain). *Landslides* https://doi.org/10.1007/s10346-016-0723-5 (2017).
118. Necsoiu, M., McGinnis, R. N. & Hooper, D. M. New insights on the Salmon Falls Creek Canyon landslide complex based on geomorphological analysis and multitemporal satellite InSAR techniques. *Landslides* **11**, 1141–1153 (2014).
119. Zhang, Y. et al. Investigating slow-moving landslides in the Zhouqu region of China using InSAR time series. *Landslides* **15**, 1299–1315 (2018).
120. Raspini, F. et al. Persistent scatterers continuous streaming for landslide monitoring and mapping: the case of the Tuscany region (Italy). *Landslides* **16**, 2033–2044 (2019).
121. Journault, J. et al. Measuring displacements of the Thompson River valley landslides, south of Ashcroft, BC, Canada, using satellite InSAR. *Landslides* **15**, 621–636 (2018).
122. Confuorto, P. et al. Monitoring of remedial works performance on landslide-affected areas through ground- and satellite-based techniques. *Catena* **178**, 77–89 (2019).
123. Raspini, F. et al. Continuous, semi-automatic monitoring of ground deformation using Sentinel-1 satellites. *Sci. Rep.* **8**, 7253 (2018).
124. Garthwaite, M. C. On the design of radar corner reflectors for deformation monitoring in multi-frequency InSAR. *Remote Sens.* **9**, 648 (2017).
125. Crosetto, M. et al. Deformation monitoring using SAR Interferometry and active and passive reflectors. *Int. Arch. Photogramm. Remote Sens. Spat. Inf. Sci.* **43**, 287–292 (2020).
126. Bovenga, F., Pasquariello, G., Pellicani, R., Refice, A. & Spilotro, G. Landslide monitoring for risk mitigation by using corner reflector and satellite SAR interferometry: the large landslide of Carlantino (Italy). *Catena* **151**, 49–62 (2017).
127. Ferretti, A. et al. Submillimeter accuracy of InSAR time series: experimental validation. *IEEE Trans. Geosci. Remote Sens.* **45**, 1142–1153 (2007).
128. Bardi, F. et al. Monitoring the rapid-moving reactivation of Earth flows by means of GB-InSAR: the April 2013 Capriglio Landslide (northern Appennines, Italy). *Remote Sens.* **9**, 165 (2017).
129. Barla, G., Antolini, F., Barla, M., Mensi, E. & Piovano, G. Monitoring of the Beauregard landslide (Aosta Valley, Italy) using advanced and conventional techniques. *Eng. Geol.* **116**, 218–235 (2010).
130. Di Traglia, F. et al. Review of ten years of volcano deformations recorded by the ground-based InSAR monitoring system at Stromboli volcano: a tool to mitigate volcano flank dynamics and intense volcanic activity. *Earth Sci. Rev.* **139**, 317–335 (2014).
131. Kromer, R. A. et al. Automated terrestrial laser scanning with near-real-time change detection-monitoring of the Séchilienne landslide. *Earth Surf. Dyn.* **5**, 293–310 (2017).
132. Catani, F. & Segoni, S. in *Treatise on Geomorphology* 2nd edn, 531–545 (Elsevier, 2021).
133. Intrieri, E., Carlà, T. & Gigli, G. Forecasting the time of failure of landslides at slope-scale: a literature review. *Earth Sci. Rev.* **193**, 333–349 (2019).
134. Hungr, O. & Kent, A. Coal mine waste dump failures in British Columbia, Canada. *Landslide News* **9**, 26–28 (1995).
135. Hutchinson, J. Landslide risk — to know, to foresee, to prevent. *Geol. Tecnica Ambientale* **9**, 3–24 (2001).
136. Gigli, G., Fanti, R., Canuti, P. & Casagli, N. Integration of advanced monitoring and numerical modeling techniques for the complete risk scenario analysis of rockslides: the case of Mt. Beni (Florence, Italy). *Eng. Geol.* **120**, 48–59 (2011).
137. Intrieri, E. & Gigli, G. Landslide forecasting and factors influencing predictability. *Nat. Hazards Earth Syst. Sci.* **16**, 2501–2510 (2016).
138. Saito, M. Forecasting time of slope failure by tertiary creep. In *Proc. 7th International Conference on Soil Mechanics and Foundation Engineering, Mexico City,* Vol. 2 677–683 (Sociedad Mexicana de Mecanica, 1969).
139. Fukuzono, T. A method to predict the time of slope failure caused by rainfall using the inverse number of velocity of surface displacement. *Landslides* **22**, 8–13 (1985).
140. Voight, B. A method for prediction of volcanic eruptions. *Nature* **332**, 125–130 (1988).
141. Kilburn, C. R. & Petley, D. N. Forecasting giant, catastrophic slope collapse: lessons from Vajont, northern Italy. *Geomorphology* **54**, 21–32 (2003).
142. Intrieri, E. et al. The Maoxian landslide as seen from space: detecting precursors of failure with Sentinel-1 data. *Landslides* **15**, 123–133 (2018).
143. Rose, N. D. & Hungr, O. Forecasting potential rock slope failure in open pit mines using the inverse-velocity method. *Int. J. Rock Mech. Min. Sci.* **44**, 308–320 (2007).
144. Carlà, T., Farina, P., Intrieri, E., Botsialas, K. & Casagli, N. On the monitoring and early-warning of brittle slope failures in hard rock masses: examples from an open-pit mine. *Eng. Geol.* **228**, 71–81 (2017).
145. Petley, D. N., Bulmer, M. H. & Murphy, W. Patterns of movement in rotational and translational landslides. *Geology* **30**, 719–722 (2002).
146. Torres, R. et al. GMES Sentinel-1 mission. *Remote Sens. Environ.* **120**, 9–24 (2012).
147. Dong, J. et al. Measuring precursory movements of the recent Xinmo landslide in Mao County, China with Sentinel-1 and ALOS-2 PALSAR-2 datasets. *Landslides* **15**, 135–144 (2018).
148. Qi, W., Yang, W., He, X. & Xu, C. Detecting Chamoli landslide precursors in the southern Himalayas using remote sensing data. *Landslides* **18**, 3449–3456 (2021).
149. Dick, G. J., Eberhardt, E., Cabrejo-Liévano, A. G., Stead, D. & Rose, N. D. Development of an early-warning time-of-failure analysis methodology for open-pit mine slopes utilizing ground-based slope stability radar monitoring data. *Can. Geotech. J.* **52**, 515–529 (2015).
150. Crosetto, M. et al. The evolution of wide-area DInSAR: from regional and national services to the European Ground Motion Service. *Remote Sens.* **12**, 2043 (2020).
151. Rosen, P. et al. The NASA-ISRO SAR (NISAR) mission dual-band radar instrument preliminary design. In *IEEE International Geoscience and Remote Sensing Symposium (IGARSS)* 3832–3835 (IEEE, 2017).
152. Kristensen, L. et al. Movements, failure and climatic control of the Veslemannen rockslide, Western Norway. *Landslides* **18**, 1963–1980 (2021).
153. Xu, Q., Yuan, Y., Zeng, Y. & Hack, R. Some new pre-warning criteria for creep slope failure. *Sci. China Technol. Sci.* **54**, 210–220 (2011).
154. Alcántara-Ayala, I. & Oliver-Smith, A. in *Identifying Emerging Issues in Disaster Risk Reduction, Migration, Climate Change and Sustainable Development* 101–124 (Springer, 2017).
155. Alcántara-Ayala, I. & Moreno, A. R. Landslide risk perception and communication for disaster risk management in mountain areas of developing countries: a Mexican foretaste. *J. Mt. Sci.* **13**, 2079–2093 (2016).
156. Intrieri, E., Gigli, G., Casagli, N. & Nadim, F. Brief communication 'Landslide early warning system: toolbox and general concepts'. *Nat. Hazards Earth Syst. Sci.* **13**, 85–90 (2013).
157. Varnes, D. J. Landslide types and processes. *Landslides Eng. Pract.* **24**, 20–47 (1958).
158. Zaruba, Q. & Mencl, V. *Landslides and Their Control* (Elsevier, 1969).
159. Aleotti, P. A warning system for rainfall-induced shallow failures. *Eng. Geol.* **73**, 247–265 (2004).
160. Van Asch, T. W. J., Buma, J. & Van Beek, L. P. H. A view on some hydrological triggering systems in landslides. *Geomorphology* **30**, 25–32 (1999).
161. Zêzere, J. L., Trigo, R. M. & Trigo, I. F. Shallow and deep landslides induced by rainfall in the Lisbon region (Portugal): assessment of relationships with the North Atlantic Oscillation. *Nat. Hazards Earth Syst. Sci.* **5**, 331–344 (2005).
162. Varnes, D. J. Slope movement types and processes. *Spec. Rep.* **176**, 11–33 (1978).
163. Hungr, O., Leroueil, S. & Picarelli, L. The Varnes classification of landslide types, an update. *Landslides* **11**, 167–194 (2014).
164. Carlà, T. et al. Rockfall forecasting and risk management along a major transportation corridor in the Alps through ground-based radar interferometry. *Landslides* **16**, 1425–1435 (2019).

Author contributions

N.C. coordinated and revised the work and provided the funding. E.I. contributed to the writing, revised the paper, coordinated revisions and prepared some of the figures. G.G. contributed to the writing, revised the paper and prepared some of the figures. V.T. contributed to the writing and revised the paper. F.R. contributed to the writing and one of the figures and revised the paper. All authors contributed to the definition and structure of the article.

Competing interests

The authors declare no competing interests.

Additional information

Correspondence should be addressed to Emanuele Intrieri.

Peer review information *Nature Reviews Earth & Environment* thanks Michel Jaboyedoff and the other, anonymous, reviewer(s) for their contribution to the peer review of this work.